Journal of Power Sources 193 (2009) 116–121

Contents lists available at ScienceDirect

Journal of Power Sources

journal homepage: www.elsevier.com/locate/jpowsour

The synthesis and characterization of the $Sm_{0.5}Sr_{0.5}Co_{1-x}Cu_xO_{3-\delta}$ cathode by the glycine–nitrate process

I-Ming Hung[a,*], Kuan-Zong Fung[b], Chung-Ta Lin[b], Min-Hsiung Hon[b]

[a] Yuan Ze Fuel Cell Center/Department of Chemical Engineering and Materials Science, Yuan Ze University, No. 135, Yuan-Tung Road, Chungli, Taoyuan 320, Taiwan
[b] Department of Materials Science and Engineering, National Cheng Kung University, No. 1, Dashiue Road, Tainan 701, Taiwan

ARTICLE INFO

Article history:
Received 15 October 2008
Received in revised form 17 November 2008
Accepted 17 November 2008
Available online 28 November 2008

Keywords:
Solid oxide fuel cell
Cathode
$Sm_{0.5}Sr_{0.5}Co_{0.8}Cu_{0.2}O_{3-\delta}$
Conductivity
Overpotential

ABSTRACT

In this study, a new oxygen-deficient cathode material, $Sm_{0.5}Sr_{0.5}Co_{1-x}Cu_xO_{3-\delta}$ (SSCCu) was developed. It is expected to enhance the efficiency of intermediate-temperature solid oxide fuel cells (IT-SOFCs). The structure, conductivity and electrochemical performance of SSCCu were examined as a function of copper content. The structure of $Sm_{0.5}Sr_{0.5}Co_{0.9}Cu_{0.1}O_{3-\delta}$ and $Sm_{0.5}Sr_{0.5}Co_{0.8}Cu_{0.2}O_{3-\delta}$ samples was a single orthorhombic perovskite phase. Second phase $SrCoO_{2.8}$, however, formed in the $Sm_{0.5}Sr_{0.5}Co_{0.7}Cu_{0.3}O_{3-\delta}$ and $Sm_{0.5}Sr_{0.5}Co_{0.6}Cu_{0.4}O_{3-\delta}$ samples. The conductivity of the $Sm_{0.5}Sr_{0.5}Co_{0.7}Cu_{0.3}O_{3-\delta}$ cathode was higher than that of other samples. However, the $Sm_{0.5}Sr_{0.5}Co_{0.8}Cu_{0.2}O_{3-\delta}$ electrode exhibited the lowest overpotential of 25 mV at 400 mA cm^{-2} and the lowest area special resistance of 0.2 Ω cm^2 at 700 °C.

1. Introduction

Solid oxide fuel cells (SOFCs) are devices that convert chemical energy into heat and electricity directly without involving combustion cycles. Compared with traditional energy technology, SOFCs have many advantages, such as high-energy conversion efficiency, high power density, low pollution and flexibility in using hydrocarbon fuels [1]. Conventional SOFCs operate at high temperature of around 800–1000 °C. However, this has many disadvantages, including that there are chemical reactions between components, only expensive ceramic conductor can be used as interconnectors, a long warm-up duration, etc. If the operation temperature of SOFCs can be decreased to 600–800 °C, the inexpensive stainless steel could be used as the interconnector, thus the chemical and thermal durability of all the components would be enhanced. However, the conductivity of the cathode material will decrease and the activation polarization of cathode electrode will obviously increase at low temperatures. Therefore, the development of high performance cathode materials is quite an important issue for intermediate-temperature SOFCs (IT-SOFC).

Perovskite-type oxides such as $La_{1-x}Sr_xMnO_3$ (LSM) [2] and $La_{1-x}Sr_xCoO_3$ (LSC) [3] and related materials have been widely studied and used as cathode materials for SOFC. The high catalytic activity of LSC is much higher than that of LSM due to its high ionic conductivity and high oxygen vacancy concentration, which enables the migration of dissociatively, adsorbed oxygen in the bulk LSC in addition to the surface diffusion route. In recent years, many reports have indicated that $Sm_{1-x}Sr_xCoO_3$ (SSC) exhibited higher catalytic activity and lower overpotential than LSC [4–6]. Fukunaga et al. have proposed a reaction model for dense SSC [7]. The result shows that adsorption–desorption at the surface of the electrode is the rate-determining step that is the same as for LSC. The adsorption and desorption rate constants of SSC were approximately one order of magnitude larger than the corresponding values of LSC. In addition, SSC is compatible both chemically and physically with ceria-based electrolyte.

In this study, a new oxygen-deficit cathode material $Sm_{0.5}Sr_{0.5}Co_{1-x}Cu_xO_{3-\delta}$ (SSCCu) was synthesized by the glycine–nitrate method. Structure, conductivity, interfacial resistance and overpotential of the SSCCu cathode were investigated.

2. Experimental

$Sm_{0.5}Sr_{0.5}Co_{1-x}Cu_xO_{3-\delta}$ ($x = 0$–0.4) powders were prepared by the glycine–nitrate process (GNP) [8]. The GNP precursor solution was prepared from the stoichiometric amount of $Sm(NO_3)\cdot 6H_2O$, $Sr(NO_3)_2$, $Co(NO_3)_2\cdot 6H_2O$, $Cu(NO_3)_2\cdot 1.5H_2O$. These metal ions sources were dissolved in distilled water. The Cu content was 0, 0.1, 0.2, 0.3 and 0.4 mol% (designed as SSC, SSCCu01, SSCCu02, SSCCu03 and SSCCu04, respectively). The mole ratio of glycine to NO_3^- was 0.5. Each solution was heated on a hotplate at 100 °C and stirred until water was evaporated and a sticky gel appeared; this resulted

* Corresponding author. Tel.: +886 3 4638800x2569 fax: +886 3 4630634.
E-mail address: imhung@saturn.yzu.edu.tw (I.-M. Hung).

0378-7753/$ – see front matter © 2008 Elsevier B.V. All rights reserved.
doi:10.1016/j.jpowsour.2008.11.081

in rapid and self-sustaining combustion. The resultant ash was then calcined at 1000 °C for 4 h in air to form the SSCC phase of the perovskite structure.

The thermogravimetry and differential thermal analysis (TG/DTA, Setaram, Setsys Evolution) was performed from room temperature to 1000 °C in air at a rate of 5 °C min^{-1}. The phase identification of the SSCCu powders was performed with a powder diffractometer (LabX, XRD-6000) with Ni-filtered Cu Kα radiation, and a diffraction angle from 20° to 80° with a step of 0.01° and a rate of 1° min^{-1}. The conductivity of the electrode was measured with the DC 4 terminal method in air using Agilent 34970A and Agilent 6645A, from 450 to 800 °C. DC measurements were carried out to measure overpotential of the SSCCu electrode using the current-interruption method. The cell based on a 12 mm diameter pellet of $Ce_{0.8}Sm_{0.2}O_{1.9}$ (SDC) electrolyte with thickness of about 0.5 mm. The cathode powders were mixed with ethylcellulose binder and screen printed on one side of SDC electrolyte. The reference Pt electrode was placed 5 mm from the cathode. On the other side of the SDC disk, the Pt counter electrode was placed symmetrically to the cathode side. The electrochemical impedance spectroscopy (EIS) was measured by potentiostat (Solartron 1287) and a frequency analyzer (Solartron 1255B/1255) from 0.1 to 1 MHz with an applied AC signal of 10 mV. The morphologies of the sintered cathode electrode were observed by field emission scanning electron microscopy (FE-SEM, Jeol 6701F).

3. Results and discussion

Fig. 1 shows the DTA/TG thermal analysis of the SSCCu01 precursor. It was found that there is a violently exothermic reaction at 170 °C, which is accompanied by 85% weight loss. This is due to the rapid and self-sustaining combustion of the precursor.

The XRD patterns of SSC sample calcined at various temperatures are shown in Fig. 2. It was found that the orthorhombic perovskite start formed as the calcination temperature increased to 800 °C. As the calcination temperature increased to 1000 °C, a single orthorhombic perovskite formed with good crystallization. Fig. 3 shows the XRD patterns of SSCCu01, SSCCu02, SSCCu03 and SSCCu04 samples calcined at 1000 °C for 4 h. The structure of the $Sm_{0.5}Sr_{0.5}Co_{0.9}Cu_{0.1}O_{3-\delta}$, $Sm_{0.5}Sr_{0.5}Co_{0.8}Cu_{0.2}O_{3-\delta}$ and $Sm_{0.5}Sr_{0.5}Co_{0.7}Cu_{0.3}O_{3-\delta}$ samples was single orthorhombic perovskite phase (JCPDS 53-0112). Second phase $SrCoO_{2.8}$ (JCPDS 39-1084), however, formed in the $Sm_{0.5}Sr_{0.5}Co_{0.6}Cu_{0.4}O_{3-\delta}$ samples. It was found that the crystallization of samples increased as copper content increased due to the decrease in the melting point of the sample with the increase in the doping amount of Cu.

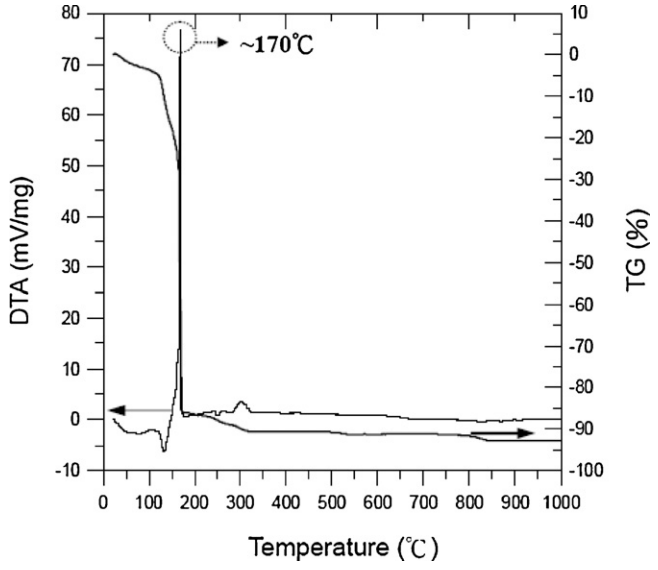

Fig. 1. TG/DTA curve of the SSCCu01 precursor with a heating rate of 5 °C min^{-1} in air.

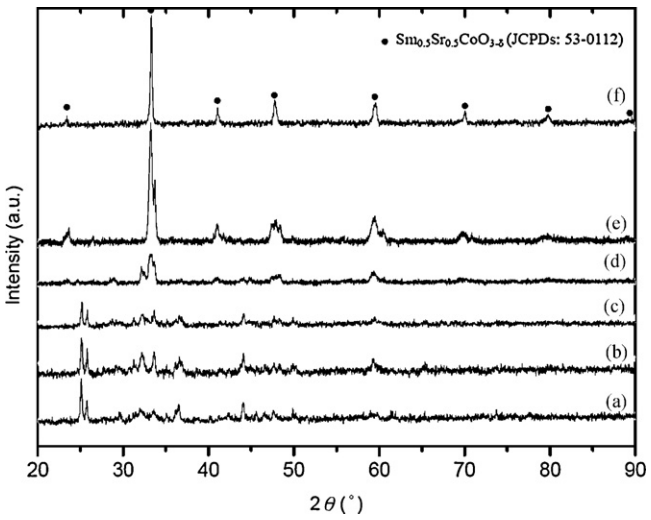

Fig. 2. XRD patterns of SSC calcined at temperature of (a) 200 °C, (b) 300 °C, (c) 400 °C, (d) 600 °C, (e) 800 °C and (f) 1000 °C for 12 h in air.

High electronic conductivity is important because it may result in a good current-collecting efficiency and a low ohmic resistance for a cathode electrode of IT-SOFC. It is well known that there are electronic and ionic conductivity mechanism in a mixed ionic and electronic conductor (MIEC), due to the co-presence of holes and oxygen vacancies. However, the ionic conductivity is much lower than the electric conductivity. Therefore, the conductivity measured with the DC 4 terminal method in this study can be believed to occur by the hopping of p-type polarons and associated with the behaviors of the triple and tetravalent state Co and Cu cations [9,10]. The temperature dependence of the total electrical conductivity of all SSCCu samples in air is given in Fig. 4. It was found that the conductivity of SSC, SSCCu01, SSCCu02 and SSCCu03 samples

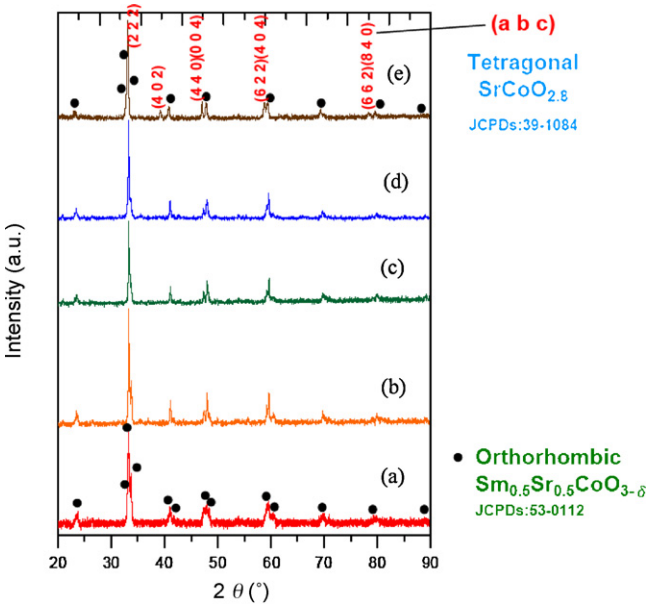

Fig. 3. XRD patterns of (a) SSC, (b) SSCCu01, (c) SSCCu02, (d) SSCCu03 and (e) SSCCu04 samples calcined at 1000 °C for 4 h in air.

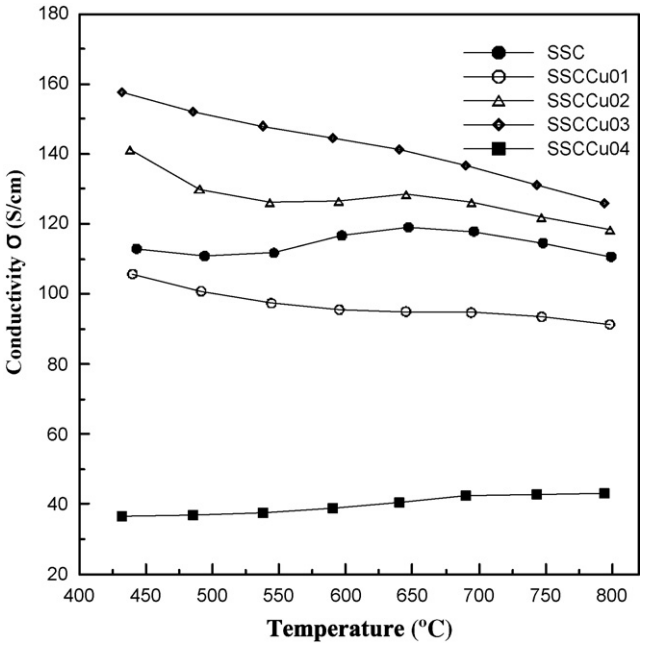

Fig. 4. Conductivity of SSC, SSCCu01, SSCCu02, SSCCu03 and SSCCu04 samples at various temperatures.

decreased with the temperature increase; this is typical behavior of an electronic conductor that depends on temperature. However, the conductivity of the SSCCu04 sample slightly increased with temperature increase; this is due to the partial ionic conductivity. The conductivity of SSCCu02 and SSCCu03 samples is higher than that of SSC, SSCCu01 and SSCCu04. At 800 °C, the highest electrical conductivity was SSCCu03, at 126 S cm^{-1}. SSCCu04 has such a low conductivity due to the large amount of second phase $SrCoO_{2.8}$ that is formed. The logarithm of electrical conductivity versus reciprocal temperature of $Sm_{0.5}Sr_{0.5}Co_{1-x}Cu_xO_{3-\delta}$ (x = 0–0.4) is plotted (as $\ln \sigma T$ versus $1/T$) in Fig. 5. The calculated activation energy of SSC, SSCCu01, SSCCu02, SSCCu03 and SSCCu04 sample is 4.3, 4.9, 4.9, 1.5 and 10.6 kJ mol^{-1}, respectively.

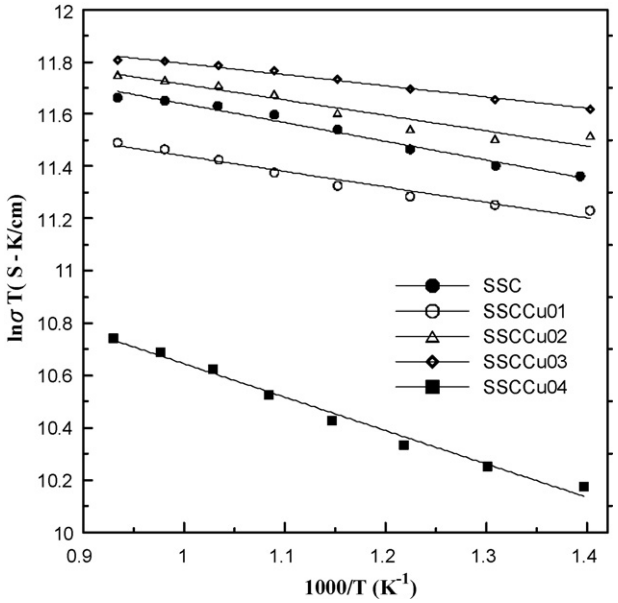

Fig. 5. Arrhenius plot of conductivity of SSC, SSCCu01, SSCCu02, SSCCu03 and SSCCu04 samples.

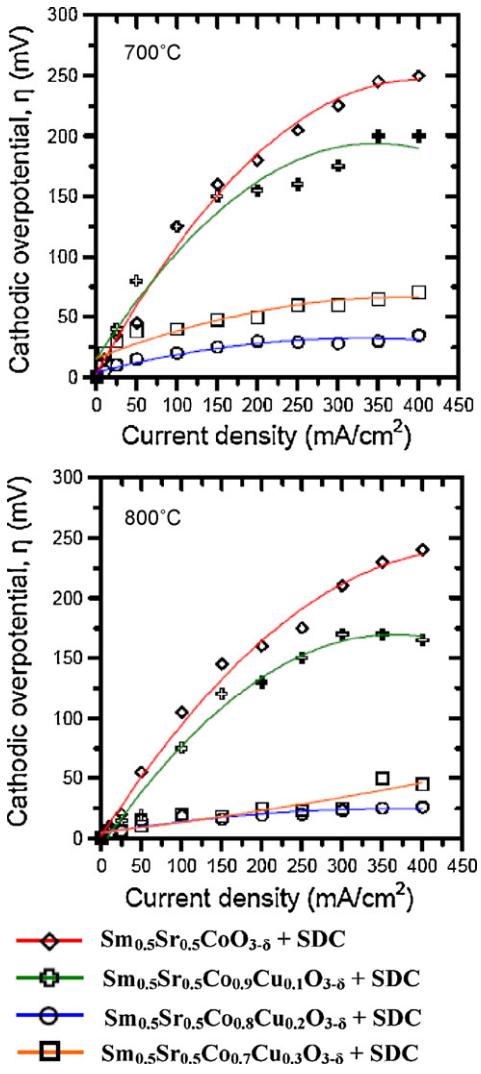

Fig. 6. Overpotential of $Sm_{0.5}Sr_{0.5}Co_{1-x}Cu_xO_{3-\delta}$ (x = 0–0.3) mixed with 30 wt% SDC cathode electrodes as function of current density at 700 and 800 °C.

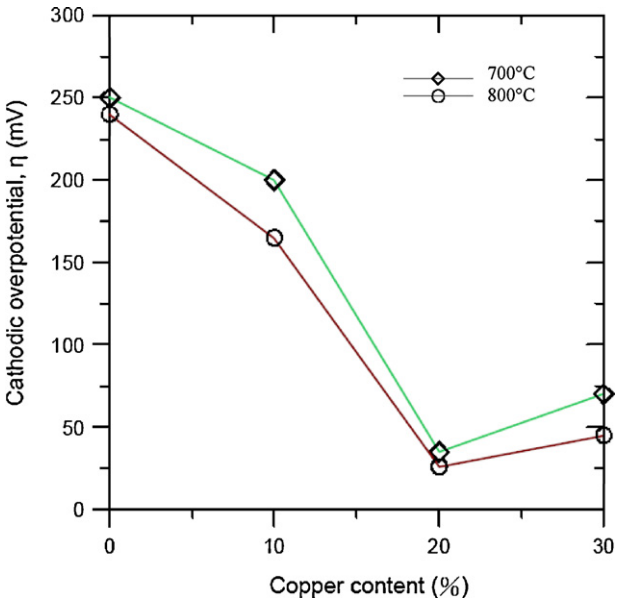

Fig. 7. Overpotential of $Sm_{0.5}Sr_{0.5}Co_{1-x}Cu_xO_{3-\delta}$ (x = 0–0.3) mixed with 30 wt% SDC cathode electrodes at current density of 400 mA cm^{-2} at 700 and 800 °C.

The overpotential of SSCCu electrodes at 700 and 800 °C with different current densities is shown in Fig. 6. For SSC and SSCCu01 samples, the overpotential increases with current density increases in the range of 0–250 mA cm^{-2}, and reaches a stable value of 250 and 190 mV, respectively, as the current density increases to 400 mA cm^{-2}. For SSCCu02 sample, the overpotential only slightly increases from 0 to 25 mV as the current density increase to 200 mA cm^{-2} and reaches a stable value. The overpotential does not increase with current density increase up to 400 mA cm^{-2}. The overpotential behavior of the SSCCu03 sample is similar to that of SSCCu02, but the maximum overpotential is 65 mV at 400 mA cm^{-2} at 700 °C. It was found that the overpotential of SSCCu02 is much lower than that of the SSC, SSCCu01 and SSCCu03 samples. A comparison of the overpotential of all samples measured at 700 °C and

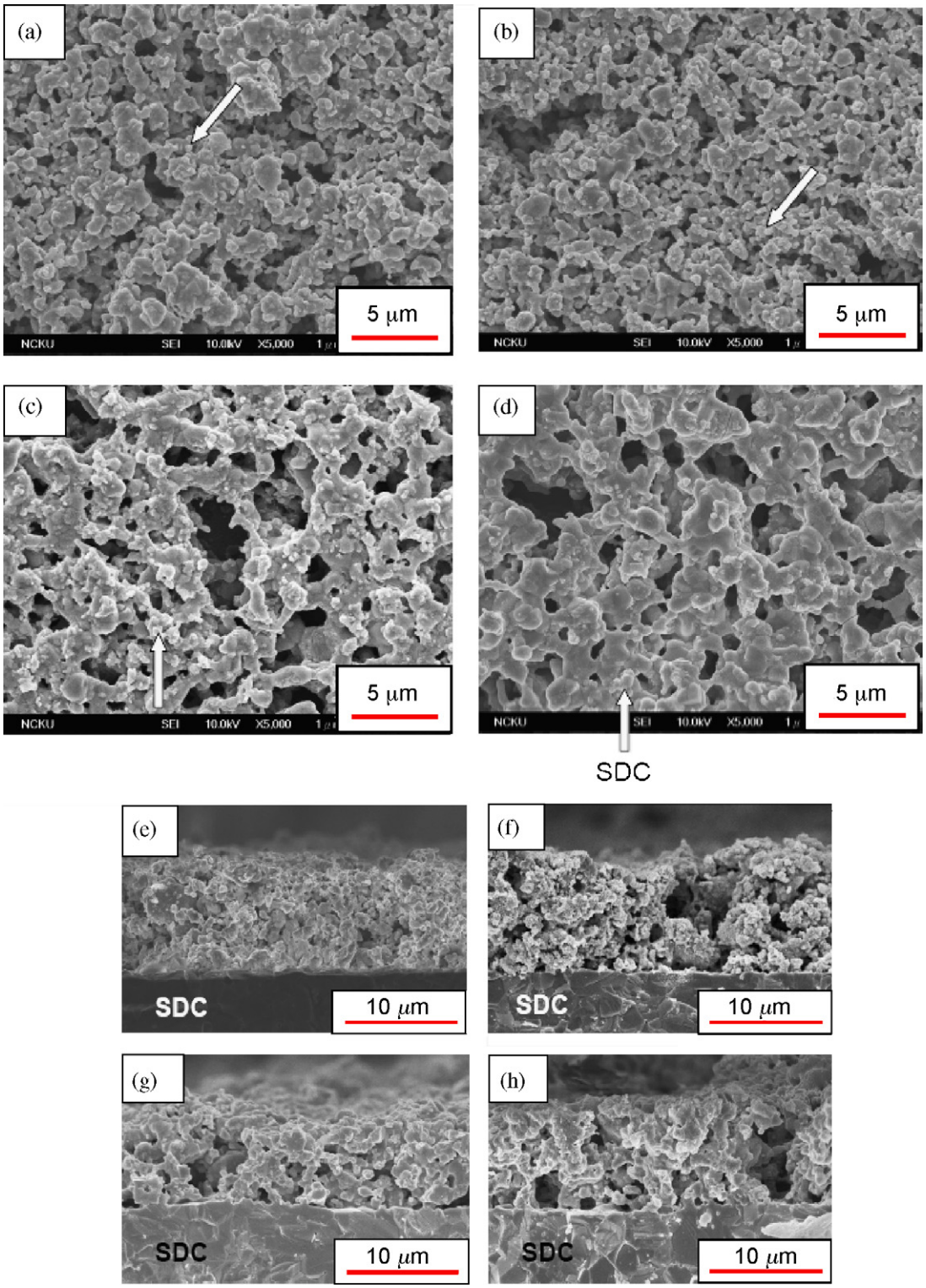

Fig. 8. SEM micrographs of top view for SSCCu-SDC cathode: (a) SSC, (b) SSCCu01, (c) SSCCu02, and (d) SSCCu03 and cross-section view for SSCCu-SDC cathode: (e) SSC, (f) SSCCu01, (g) SSCCu02, and (h) SSCCu03 sintered at 1000 °C for 4 h.

800 °C is shown in Fig. 7. It was found that the overpotential increase behavior is similar, but the maximum overpotential data of samples measured at 800 °C is lower than that measured at 700 °C by about 10–50 mV. It is well agreed that the oxygen electro-reduction process in a cathode electrode is a multistep electrochemical process, including: (1) diffusion of O_2 from the gas phase to the surface of the cathode; (2) dissociation of chemisorbed oxygen molecules into atomic oxygen at the active site; (3) charge transfer; (4) diffusion of O^{2-} from the cathode electrode to cathode/electrolyte interface and into the electrolyte [11]. It is suggested that the low overpotential behavior of SSCCu02 is due to the high oxygen vacancy concentration [12]. The activation polarization of the cathode electrode at low temperatures is mainly due to the dissociation rate of chemisorbed oxygen molecules and oxygen diffusion [13,14]. In order to retain the electrical neutrality, the reduction of the Co and Cu ions is expected occur; this can be described in Eqs. (1) and (2), respectively:

$$2Co_{Co}\cdot + O_o{}^x \leftrightarrow 2Co_{Co}{}^x + Vo\cdot\cdot + (1/2)O_2 \quad (1)$$

$$2Cu_{Cu}\cdot + O_o{}^x \leftrightarrow 2Cu_{Cu}{}^x + Vo\cdot\cdot + (1/2)O_2 \quad (2)$$

The area of chemisorbed oxygen and the oxygen diffusion rate and path were enhanced by the high concentration of oxygen vacancy in the SSCCu02 sample. Therefore, the overpotential is lower than that of other samples especially at high current density.

The microstructure of the SSCCu-SDC electrodes top view and cross-sections were observed by SEM. Typical images are shown in Fig. 8. It was found that the grain size and pore size of SSCCu samples increased with the Cu doping amount, especially in the SSCCu02 and SSCCu03 sample. This is because the melting point of SSCCu samples decreases when the Cu doping amount increases. The thickness of all cathode electrodes was approximately 10 μm. Both SSC-SDC and SSCCu-SDC cathode electrodes exhibited good interfacial contact with the SDC electrolyte; no delamination was observed.

The activation polarization of the cathode electrode due to charge transfer occurred in the interface between the cathode and the electrolyte. The cathode performance was investigated by the EIS technique based on symmetrical cells. The EIS for the SSC, SSCCu01, SSCCu02 and SSCCu03 cathode electrodes on the SDC electrolyte recorded at 700 °C in air are shown in Fig. 9. It can be seen that the ASR of SSCCu is obviously lower than that of the SSC electrode. The ASR of SSC, SSCCu01, SSCCu02 and SSCCu03 electrode is 11.3, 7.3, 0.2 and 0.5 Ω cm^2, respectively. The area-specific resistance versus the reciprocal temperature of SSC and SSCCu electrodes is shown in Fig. 10. The activation energy is 109, 75, 129 and 118 kJ mol^{-1}, respectively. These values are much lower than that of LSCF cathode electrode [15]. The potential resistance of the cathode electrode is closely related not only to the charge transfer and the adsorption/dissociation of oxygen, but also to the transport speed of oxide ions through the bulk and across the cathode/electrolyte

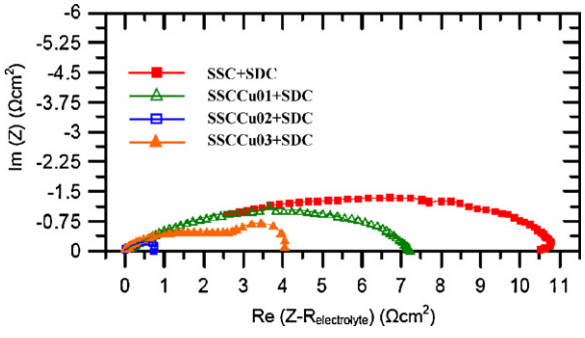

Fig. 9. Impedance spectra of different copper content for $Sm_{0.5}Sr_{0.5}Co_{1-x}Cu_xO_{3-\delta}$ (x = 0–0.3) mixed with 30 wt% SDC at 700 °C in air.

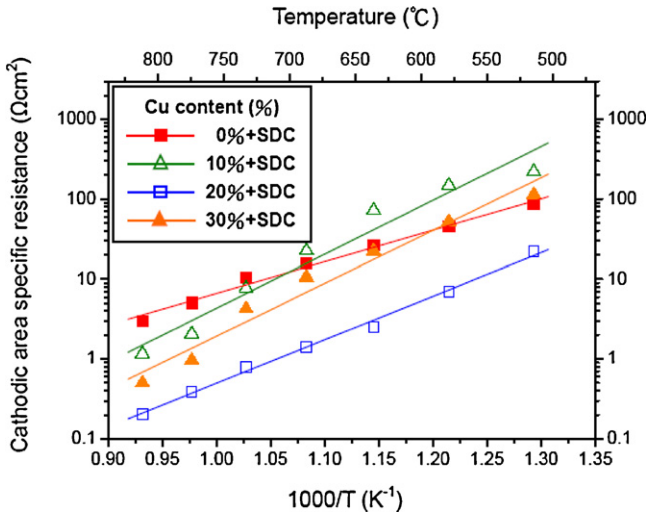

Fig. 10. Arrhenius plots of area-specific resistance of different copper content $Sm_{0.5}Sr_{0.5}Co_{1-x}Cu_xO_{3-\delta}$ (x = 0–0.3) electrodes mixed with 30 wt% SDC.

interface. Therefore, the kinetics of oxygen exchange and diffusion of oxide ions in the cathode materials as well as electronic conductivity play a critical role in the oxygen reduction reaction [16]. It is suggested that the kinetic of oxygen exchange and diffusion of oxygen in the SSCCu02 sample is higher than that in the other samples; therefore it exhibits the lowest overpotential and ASR, even though its conductivity is not the highest. For the SSCCu03 sample, a small amount of second phase start formed, so the electrochemical performance cannot be further improved. The quantification of oxygen vacancy concentration in SSCCu samples and power density of a single cell based on the SSCCu02 cathode electrode are still being researched.

4. Conclusions

$Sm_{0.5}Sr_{0.5}Co_{1-x}Cu_xO_{3-\delta}$ (x = 0–0.3) cathode materials were successfully prepared by GNP and had a stable orthorhombic perovskite structure. The $Sm_{0.5}Sr_{0.5}Co_{0.8}Cu_{0.2}O_{3-\delta}$ exhibited an acceptable conductivity of 125 S cm^{-1} at 700 °C, the lowest overpotential of 25 mV at 400 mA cm^{-2} and the lowest area special resistance of 0.2 Ω cm^2 at 700 °C. Therefore, $Sm_{0.5}Sr_{0.5}Co_{0.8}Cu_{0.2}O_{3-\delta}$ will be a promising candidate for intermediate-temperature solid oxide fuel cell cathode material.

Acknowledgement

The work was supported by the National Science Council of Taiwan (NSC 96-2221-E-155-053 and NSC 97-2221-E-155-059).

References

[1] N.Q. Minh, J. Am. Ceram. Soc. 76 (1993) 563–588.
[2] A. Hammouche, E. Siebert, A. Hammou, M. Kleitz, J. Electrochem. Soc. 138 (1991) 1212–1216.
[3] S.B. Adler, J.A. Lane, B.C.H. Steele, J. Electrochem. Soc. 143 (1996) 3554–3564.
[4] M. Godickemeier, K. Sasaki, L.J. Gauckler, I. Riess, Solid State Ionics 86 (88) (1996) 691–701.
[5] H.Y. Tu, Y. Takeda, N. Imanishi, O. Yamamoto, Solid State Ionics 100 (1997) 283–288.
[6] H.Y. Tu, Y. Takeda, N. Imanishi, O. Yamamoto, Solid State Ionics 117 (1999) 277–281.
[7] H. Fukunaga, M. Koyama, N. Takahashi, C. Wen, K. Yamada, Solid State Ionics 132 (2000) 279–285.
[8] C. Xia, F. Chen, M. Liu, Electrochem. Solid-State Lett. 4 (2001) A52–A54.
[9] S. Carter, A. Selcuk, R.J. Chater, J. Kajda, J.A. Kilner, B.C.H. Steele, Solid State Ionics 53 (56) (1992) 597–605.
[10] S. Li, Z. Lu, B. Wei, X. Huang, J. Miao, G. Cao, R. Zhu, W. Su, J. Alloy Compd. 426 (2006) 408–414.

[11] H. Uchida, M. Yoshida, M. Watanabe, J. Electrochem. Soc. 146 (1999) 1–7.
[12] B. Wei, Z. Lü, S. Li, Y. Liu, K. Liu, W. Su, Electrochem. Solid-State Lett. 8 (2005) A428–A431.
[13] S. Kim, Y.L. Yang, A.J. Jacobson, B. Abeles, Solid State Ionics 106 (1998) 189–195.
[14] H. Lv, Y.J. Wu, B. Huang, B.Y. Zhao, K.A. Hu, Solid State Ionics 177 (2006) 901–906.
[15] H.J. Hwang, J.W. Moon, S.E. Lee, A. Lee, J. Power Sources 145 (2005) 243–248.
[16] K.T. Lee, A. Manthiram, Solid State Ionics 176 (2005) 1521–1527.